1964

Effect of internal pressure on compressive buckling stress of a cylindrical shell under eccentric loading

Chao-Ping Chu

Department:

EFFECT OF INTERNAL PRESSURE ON COMPRESSIVE BUCKLING STRESS OF A CYLINDRICAL SHELL UNDER ECCENTRIC LOADING

BY

CHAO-PING CHU

A

THESIS

Submitted to the Faculty of the

UNIVERSITY OF MISSOURI AT ROLLA

in Partial Fulfillment of the Work Required for the

Degree of

MASTER OF SCIENCE IN CIVIL ENGINEERING

Rolla, Missouri

1964

Approved by

Joseph H. Senne Jr. (advisor) James S. Sawyer

H. C. Middlebrooks C. K. Remington Jr.

ABSTRACT

In this paper, an investigation was made of a thin-walled cylindrical shell under compressive load with various eccentricities and internal pressures to study the effect of the internal pressure on the compressive buckling stress of the shell.

So far, theoretical methods have not been devised to solve this problem; therefore, an experimental study was carried out. The experimental results indicated that the buckling load of the shell decreases as the eccentricity increases, that the buckling stress increases as the eccentricity increases, and that the change in buckling stress increases with an increase of internal pressure and is very nearly independent of eccentricity.

TABLE OF CONTENTS

LIST OF FIGURES

LIST OF TABLES

TABLES PAGE

ACKNOWLEDGMENT

The author wishes to express his sincere appreciation to Dr. Joseph H. Senne, Jr. and Dr. Louis G. Petro, Professor and former Professor of the Department of Civil Engineering, University of Missouri at Rolla, who gave many valuable suggestions and guidance on this problem. The author also wishes to thank James E. Spooner, Assistant Professor of Civil Engineering Department, who read the paper and gave helpful corrections. He would like to thank many of the faculty members of the Department of Mechanics for their continual supervision and helpful suggestions throughout the preparation of this paper.

SYMBOLS

E	Young's Modulus
P_{cr}	Buckling load
R_m	Radius of curvature in the meridional plane
R_t	Radius of curvature in the tangential plane
S_m	Meridional membrane stress of the shell
S_t	Tangential membrane stress of the shell
r	Radius of cylinder
l	Length of cylinder
t	Wall thickness of cylinder
e	Eccentricity of load
p	Internal pressure, psig
$\bar{p}$	$\frac{p}{E}\left[\frac{r}{t}\right]^2$
ϵ_{ucr}	Buckling strain
σ_{ucr}	Buckling stress
$\bar{\sigma}$	$\frac{\sigma}{\quad}$
$\Delta\bar{\sigma}_{ucr}$	$\bar{\sigma}_{ucr} - (\bar{\sigma}_{ucr})_{\bar{p}=0}$

Chapter I

INTRODUCTION

Since the cylindrical shell is a structural component very useful in modern aircraft and missile design, a knowledge of its true behavior is very important. Although many theoretical and experimental investigations have been carried out in this field, the results are still far from complete.

Some experimental tests (1) have shown that the buckling load is about 40% of the calculated value in longitudinal compression for thin-walled circular shells, which indicates that the classical solution should not be used for design purposes; or we may simply say that the classical method based upon the small-deflection theory is inadequate.

Many experiments have been conducted (3,4) on pressurized cylindrical shells under axial compressive load, but only a few experimental results have been reported for eccentric loading. Furthermore, since the theory for large-deflection analysis has not been adequately established, the true behavior of the pressurized cylindrical shell under eccentric loading must be predicted by experimental procedure.

In this paper, a study has been made on a thin-walled

cylindrical shell under various eccentric loads and internal pressures to investigate the effect of internal pressure on the compressive buckling stress of the shell.

Chapter II

REVIEW OF LITERATURE

Because the steel thin-walled cylindrical shell can take relatively larger amounts of tensile than compressive force, and also since the thickness of the shell is extremely small in comparison with the other dimensions, the buckling stress of the shell usually governs the design.

During early experimental work, the buckling of thin-walled cylinders under axial compression and lateral pressure was investigated by Flugge (8), who found that the effect of the internal pressure does not have a noticeable effect on the buckling stress of a cylindrical shell.

From the theoretical point of view, the small-deflection theory can apply only when the deflections are small with respect to the wall thickness "t". Since the steel sheet can have very large deflections without reaching its yield stress, the small-deflection theory does not apply to the steel sheet cylindrical shell.

Because the small-deflection theory can not be applied to the shell problem, the large-deflection theory in which the bending stress is neglected with respect to the membrane stress must be considered (2).

From this theory and Figure 1,

$$\frac{S_m}{R_m}+\frac{S_t}{R_t}=\frac{p}{t}$$

and since

$R_m=\infty$ while $R_t=r$

so,

$$S_t=\frac{pr}{t}$$

and by equilibrium

$$S_m=\frac{pr}{2t}$$

where S_m is the meridional membrane stress, S_t is the tangential membrane stress, R_m is the radius of curvature in meridional plane and is equal to ∞ for a cylindrical surface, R_t is the radius of curvature in tangential plane, p is internal pressure, t is wall thickness and r is the radius of the cylindrical shell.

First, since S_m is a tensile stress occurring in the longitudinal direction of the cylinder, it reduces the compressive stress caused by eccentric load or by both axial load and bending moment.

Second, as S_t is the tensile stress occurring along the circumferential direction of the shell, it tends to maintain the original circular shape, which is the most stable form, being more resistant to buckling loads than any other shape.

For the foregoing reasons, it should be easy to see

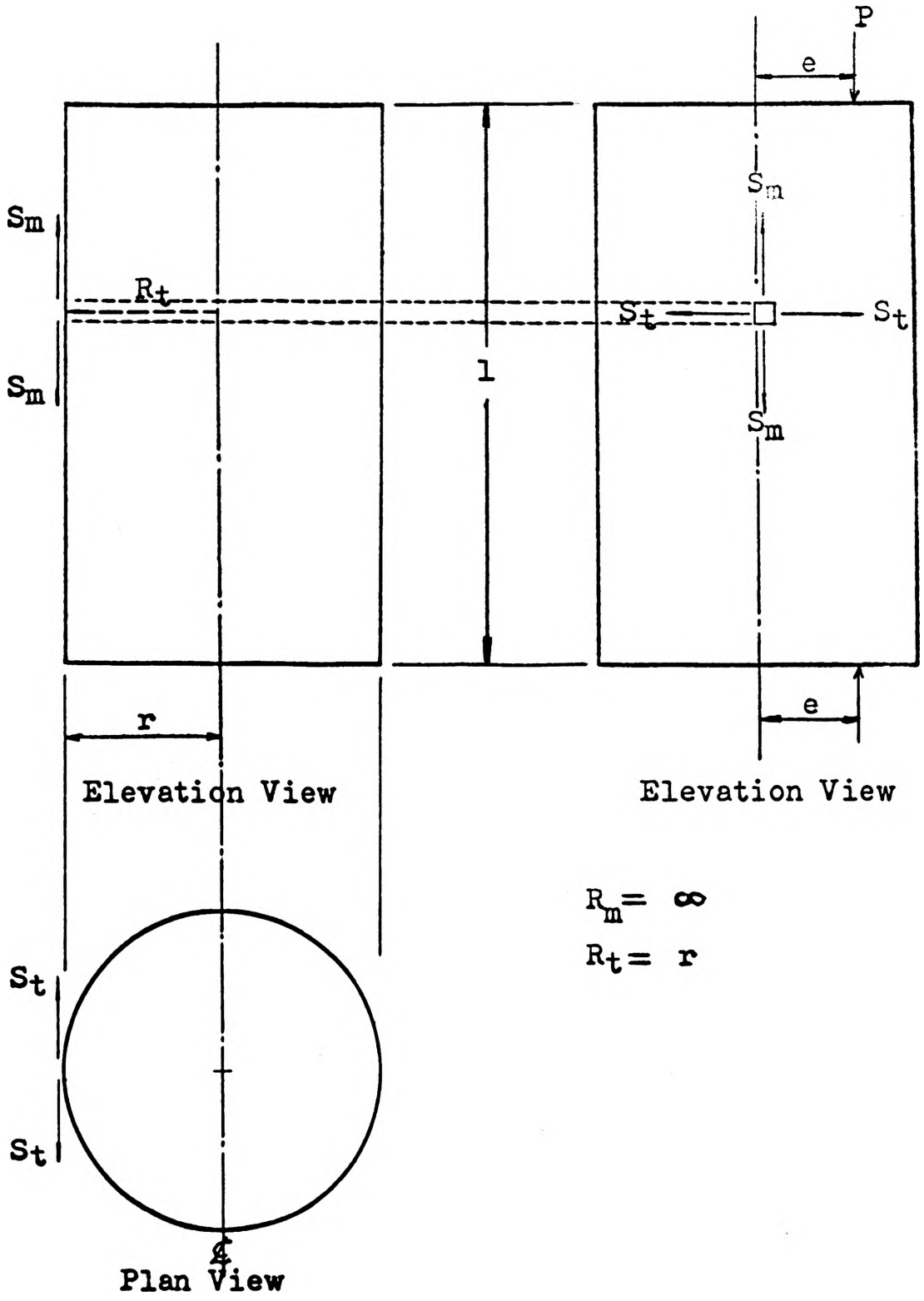

Fig. 1. Parameters of the cylindrical shell

that considerable benefit can be derived by using internal pressure to increase the resistance to buckling.

In 1942, Rafel and Norman reported in their experimental results that a certain amount of strengthening effect due to lateral pressure on the buckling load of the curved panels had been determined (6).

Both a theoretical and experimental study (3) have been reported on the effect of the internal pressure on the buckling stress of thin-walled cylinders under axial compressive loads and internal pressures. The theoretically predicted increase of compressive buckling stress due to internal pressure agrees fairly well with the experimental results, but the theoretical solution for eccentric loading still has not been determined.

A few studies of the effect of internal pressure on buckling stress of thin-walled cylinders under pure bending have been made (4, 7), but the results still seem inconclusive.

Chapter III

DISCUSSION

A. Description of Apparatus

Test Specimen: The specimen used for the tests was a cylindrical shell, 27 inches long with a 15-inch inside diameter, made of No. 28 gage galvanized steel sheet of 0.022 inch average thickness; the Young's Modulus was 30.5×10^6 psi. The butt-joint of the two longitudinal edges was covered by a strip 0.022 inch thick and 1½ inches wide, and was riveted with 1/8 inch rivets spaced 3/8 inch on center along the total length of the cylinder (Fig. 2).

Both the top and the bottom heads were made of ¼ inch A-7 steel plate and then welded to 15-inch outside diameter steel rings ¼ inch thick and 1 inch in height. These rings were used for protecting against local failure caused by the moment transferred from the heads along the edges of the cylindrical shell. On the top head, strain gage wire outlets and the air pressure inlet were provided. The wire outlets were sealed by Smooth-on No. 1 steel cement after the strain gages had been fastened on the shell. The joints between the cylinder and the heads were arc-welded using nickel rods (Figs. 3, 4). A slight leakage of air was found along these joints.

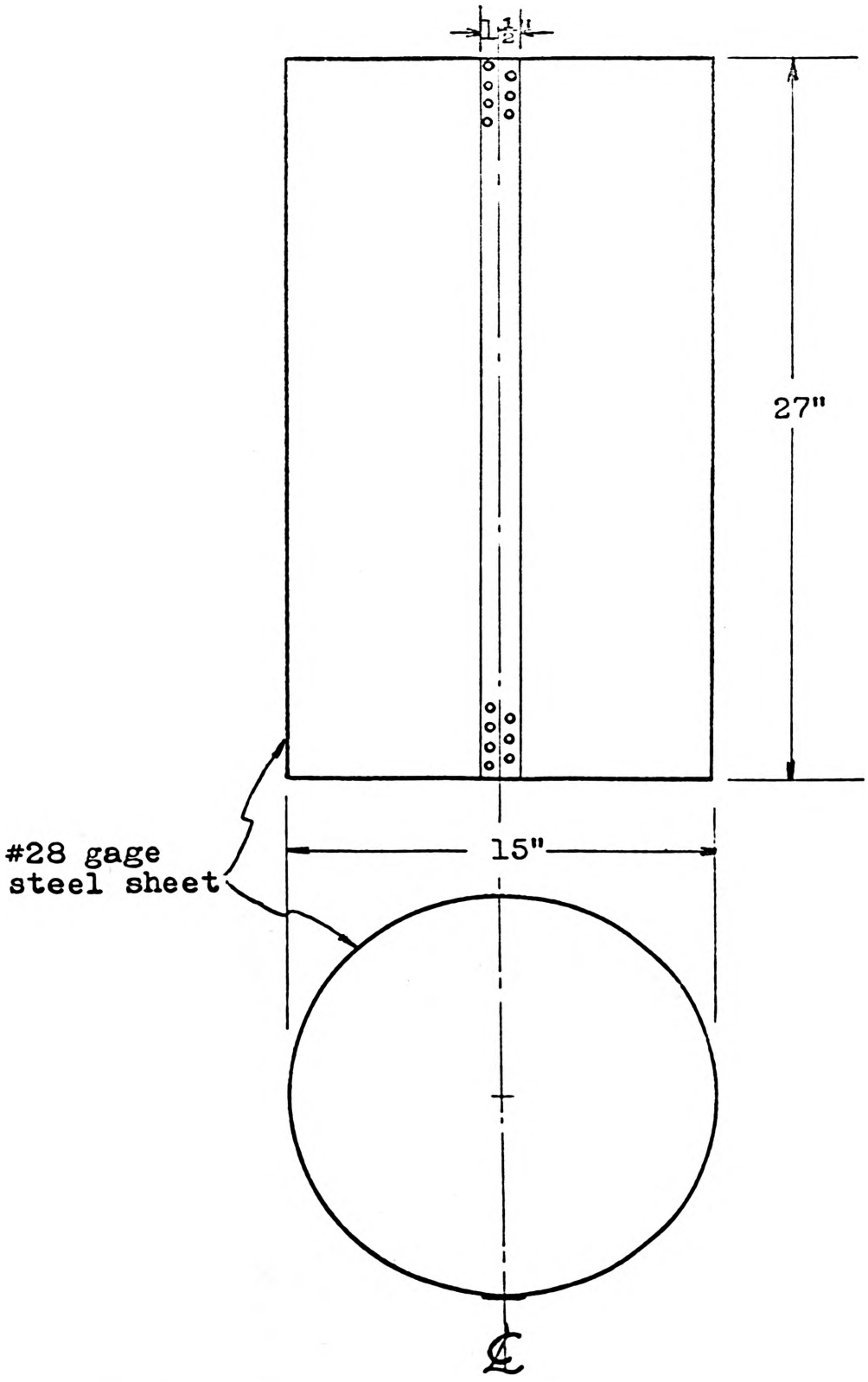

Fig. 2. Body of the cylindrical shell

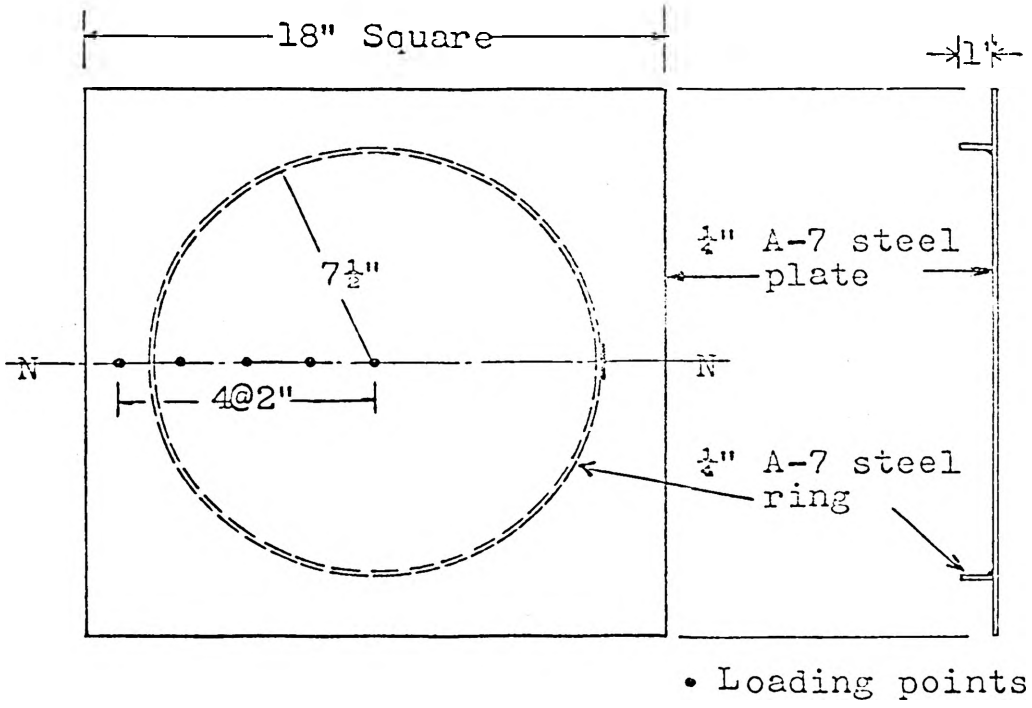

Fig. 3. Bottom head and loading point positions

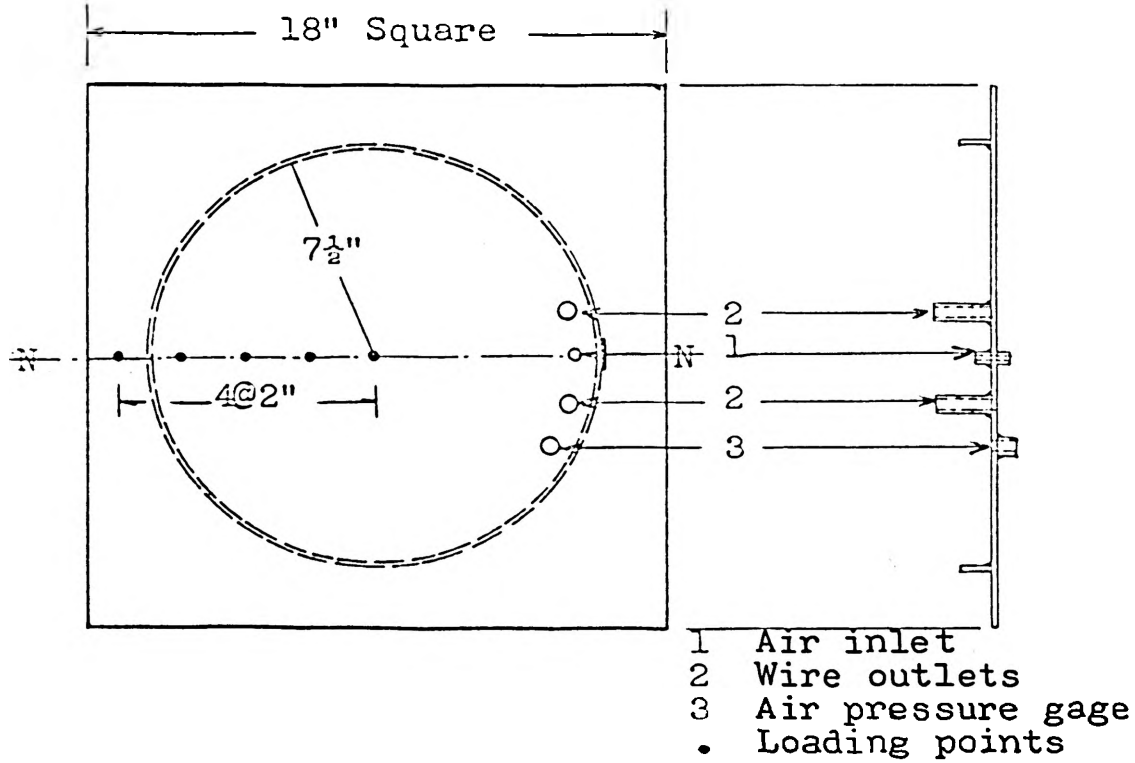

Fig. 4. Top head and loading point positions

Instrumentation: Equally spaced along the outside circumference of the cylindrical shell at mid-length were 12 SR-4 electric strain gages, and directly opposite them on the inside were 12 additional gages. Of these 24 gages, 16 were A-3 paper-base strain gages used to measure the strain along the longitudinal direction of the shell, and the other eight were AR-1 paper-base rosette strain gages for measuring both the longitudinal and circumferential strain (Fig. 5).

The strain gages were connected to the switching units, Baldwin SR-4, Badd and Arthur R. Anderson; and then connected to the Baldwin-Lima-Hamilton SR-4 strain indicators which can be read to two micro-inches per inch.

The Riehle 60,000-pound universal testing machine (with a minimum loading speed of 0.025 inch per min.) in the Testing Laboratory of the Department of Mechanics, University of Missouri at Rolla, was used.

B. Experimental Procedures

The specimen was placed in the testing machine and subjected to an eccentric compressive loading. Compressed air was used to produce internal pressure. As indicated on page 16, there was a slight leakage along the welded joints; an air regulator was installed in order to maintain the air pressure at any desired constant value. The

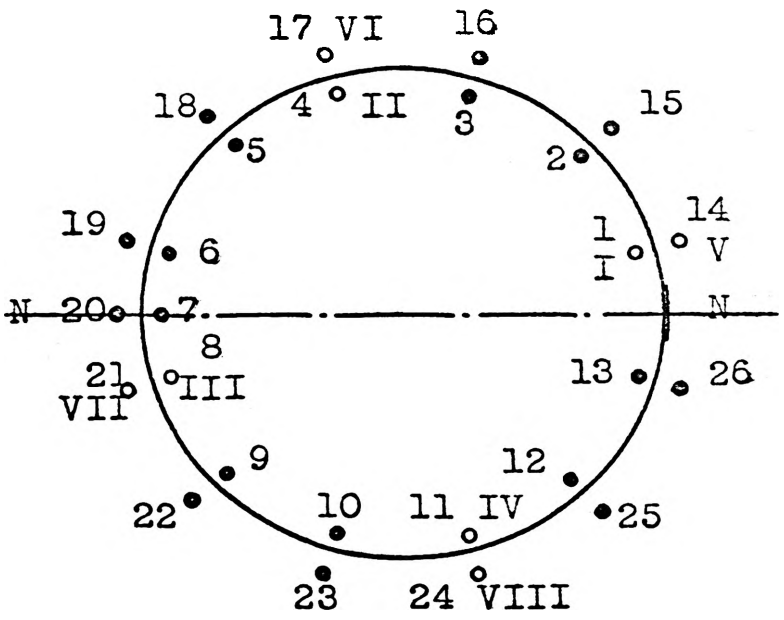

Arabic numerals denote gages measuring longitudinal strain

Roman numerals denote gages for circumferential strain

- A-3 paper-based gage
- AR-1 rosette

Fig. 5. Strain gage positions

Fig. 6. Machine set-up

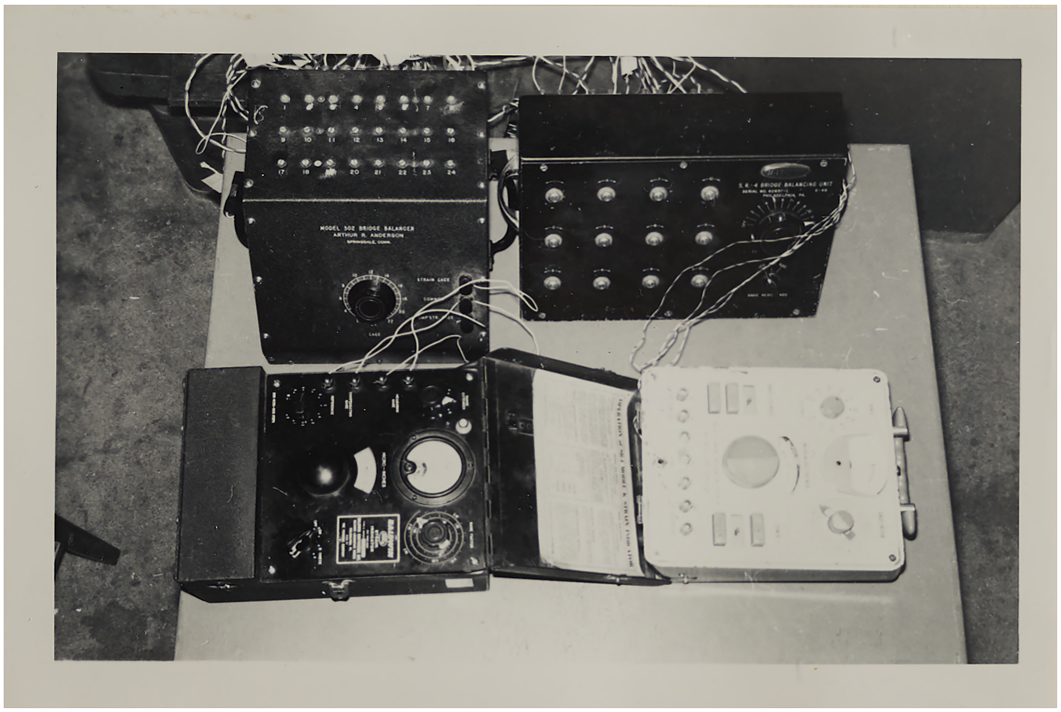

Fig. 7. Switching units and strain indicators

Fig. 8. Air regulator set-up

air pressure gage reading to one psi was used to measure the amount of internal pressure.

The switching units were first adjusted so that all the gage readings were equal. Then the compressed air was let into the cylindrical shell, and by adjusting the air regulator the desired internal pressure could be controlled to within 0.1 psi.

The eccentric compressive load was increased in increments until the buckling was observed. At each increment all gage readings were recorded. The load was next decreased until the buckle disappeared, then increased again to check the previous reading. During all these steps the internal pressure was maintained at a constant level. The load was then reduced and the internal pressure was increased by the next increment. The pressure "p" varied from 0 to 20 psig, and is shown in Table 1.

After the series of internal pressures had been applied for one load point, the eccentricity was changed to the next point along line N N and loads were applied with another series of internal pressures. For each value of eccentricity and each value of internal pressure, the same procedure of loading and recording was repeated.

C. Experimental Results

The typical experimental results are shown in Fig. 9

and in Fig. 10. In these figures the compressive load is plotted against the strain, which was calculated from the strain-gage readings within the range where the load-strain relation is linear. For the case in Fig. 9, the test results of four pairs of strain gages with the eccentricity of zero and the internal pressure of 3 psi were plotted. They indicated that the buckling occurred at a compressive load of 21,000 pounds and was located between the two pairs of strain gages, 6 & 19 and 7 & 20. Note that the strain maintained a constant value as the compressive load increased from 21,700 pounds to 21,900 pounds. This phenomenon was considered to be the buckling of the shell and the corresponding load to be the buckling load "P_{cr}". In Fig. 10, the load-strain relation of the three pairs of strain gages at an eccentricity of 6 inches and the internal pressure of 3 psi is shown. In this case only one pair of strain gages, 7 & 20, had reached the buckling load, 8,400 pounds.

The local buckling stress "σ_{ucr}" is the corresponding value of the buckling strain "ϵ_{ucr}" and can be found from the Young's Modulus of the material used.

For every value of internal pressure applied, the buckling occurred at gages 7 & 20 for all values of eccentricity except that of zero, which occurred between gages 6 & 19 and 7 & 20. The point of buckling was determined

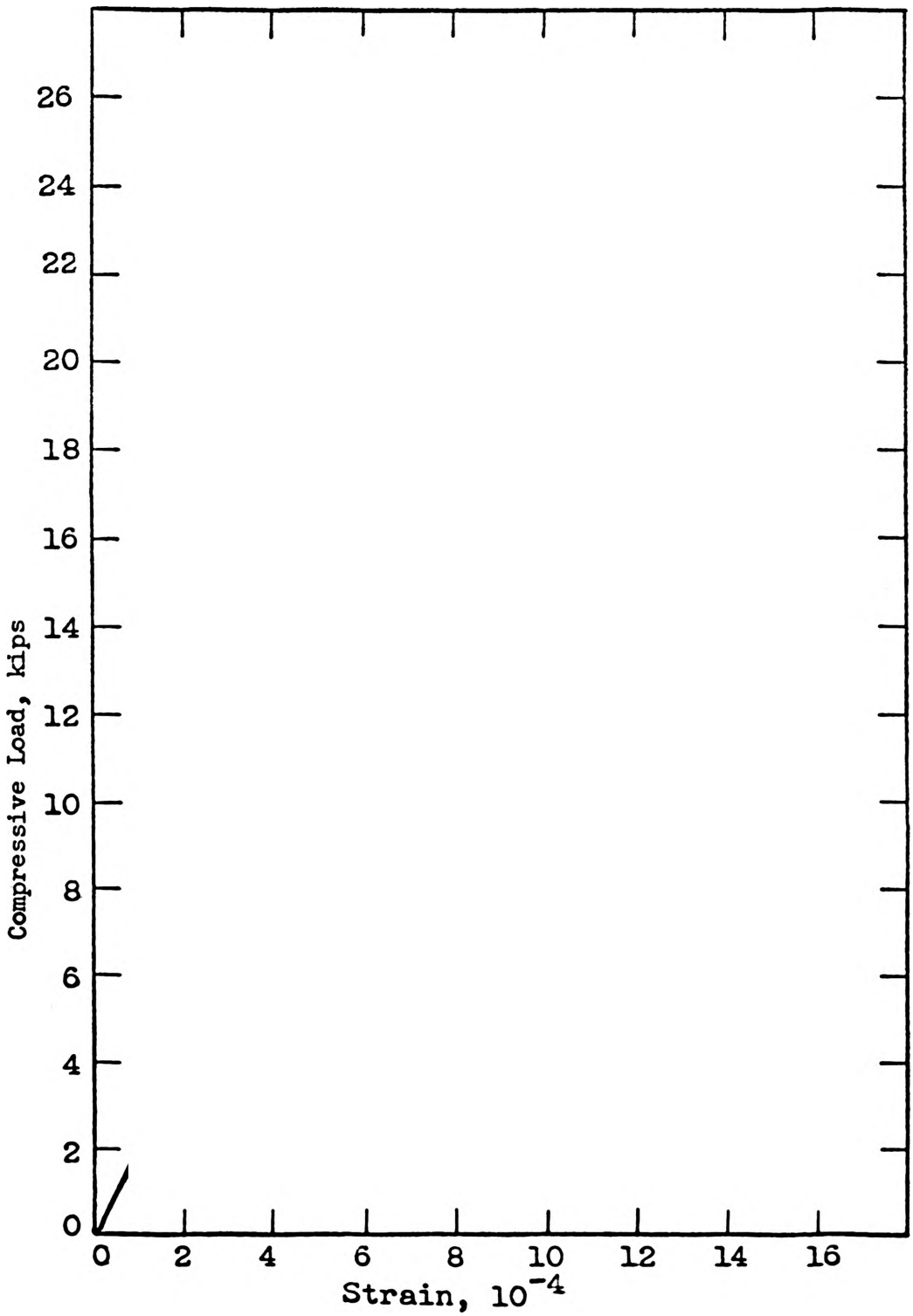

Fig. 9. Linear part of the load-strain curve for four typical pairs of strain gages including the two pairs in which buckling occurred (e = 0", p = 3psi)

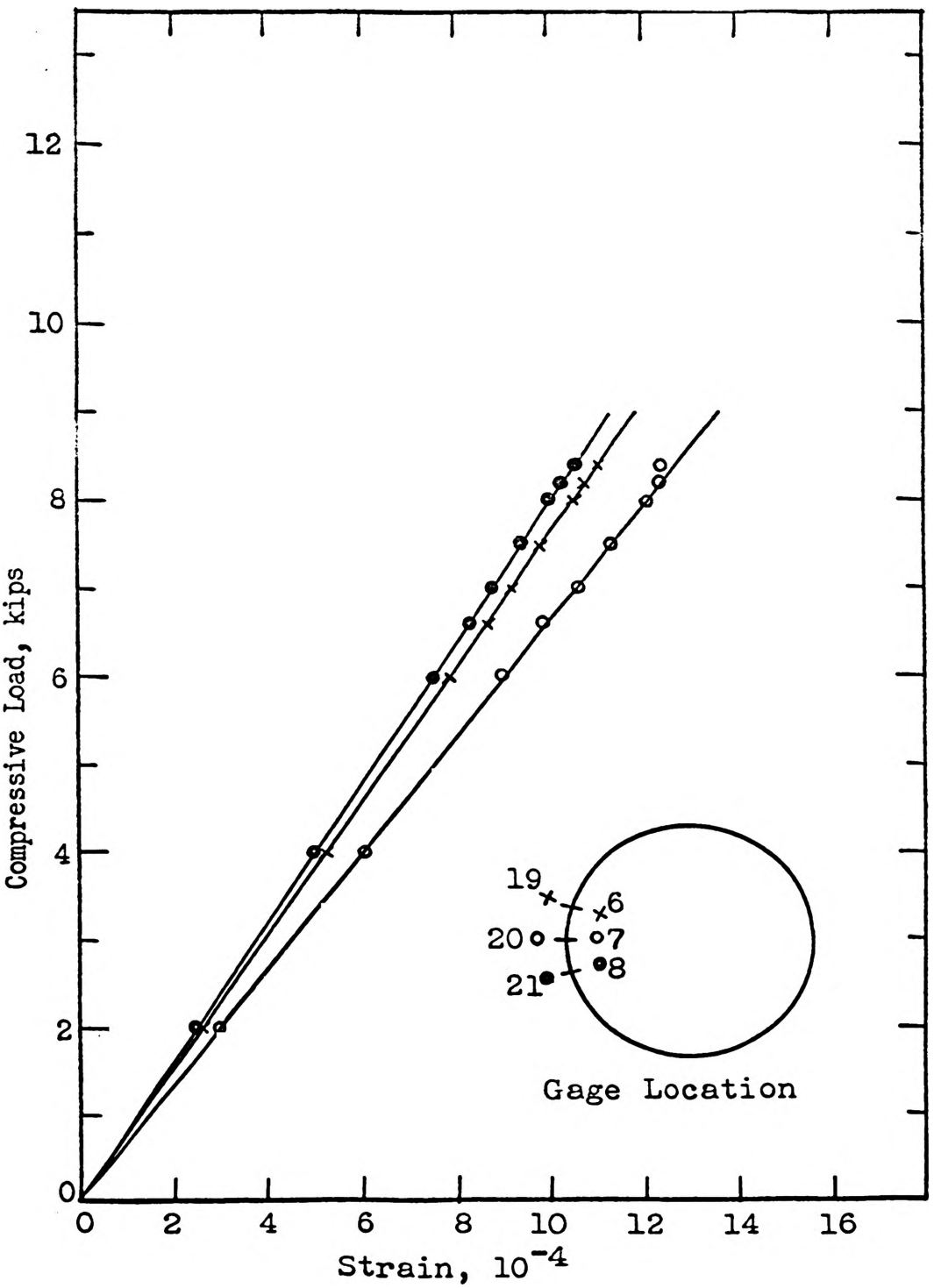

Fig. 10. Linear part of the load-strain curve for three typical pairs of strain gages including the one pair in which buckling occurred (e= 6", p = 3 psi)

only when a large strain occurred in one of the gages. No visible evidence of buckling could be observed.

The results for each value of eccentricity and internal pressure are tabulated in Table I and plotted in Fig. 11 in terms of P_{cr} and p. The results are also plotted in Fig. 12 in terms of two non-dimensional parameters:

$$\bar{\sigma}_{ucr} = \frac{\sigma_{ucr}}{E} \frac{r}{t}$$

$$\bar{p} = \frac{p}{E}\left(\frac{r}{t}\right)^2$$

The typical stress distribution curve is plotted in Fig. 13 by using the longitudinal stresses of all gages when $e = 6"$ while $p = 5$ psi.

Stresses in the circumferential direction of the shell increased as pressurization took place and varied only a small amount during testing.

TABLE I — Buckling stresses for various internal pressures at different eccentricities

e in	p psi	$\bar{p}$	P_{cr} kips	ϵ_{ucr} 10^{-6}	$\bar{\sigma}_{ucr}$	$\Delta\bar{\sigma}_{ucr}$	$p\pi r^2$ lbs	Remarks
0	0	.0000	18.6	874	.2980	.0000	0.0	buckling
0	1	.0038	20.0	939	.3202	.0222	176.8	occurred
0	2	.0076	20.6	967	.3299	.0319	353.6	between
0	3	.0114	21.9	1,030	.3511	.0531	530.4	strain
0	4	.0152	22.3	1,044	.3561	.0581	707.2	gages
0	5	.0190	23.1	1,087	.3707	.0727	884.0	6 & 19
0	8	.0304	24.3	1,128	.3847	.0867	1,414.4	and
0	12	.0456	25.7	1,211	.4132	.1152	2,121.6	7 & 20
0	16	.0608	27.1	1,288	.4393	.1413	2,828.8	
0	20	.0760	28.1	1,324	.4515	.1535	3,536.0	

TABLE I — Continued

e in	p psi	$\bar{p}$	P_{cr} kips	ϵ_{ucr} 10^{-6}	$\bar{\sigma}_{ucr}$	$\Delta\bar{\sigma}_{ucr}$	$p\pi r^2$ lbs	Remarks
4	0	.0000	9.4	943	.3216	.0000	0.0	buckling
4	1	.0038	10.0	1,007	.3433	.0217	176.8	occurred
4	2	.0076	10.5	1,041	.3551	.0335	353.6	at gages
4	3	.0114	11.2	1,126	.3840	.0624	530.4	7 & 20
4	4	.0152	11.4	1,144	.3900	.0684	707.2	
4	5	.0190	11.7	1,175	.4008	.0792	884.0	
4	8	.0304	12.1	1,223	.4170	.0954	1,414.4	
4	12	.0456	12.8	1,296	.4420	.1204	2,121.6	
4	16	.0608	13.7	1,379	.4702	.1486	2,828.8	
4	20	.0760	14.0	1,411	.4812	.1596	3,536.0	
6	0	.0000	7.4	1,098	.3744	.0000	0.0	buckling
6	1	.0038	7.8	1,157	.3946	.0202	176.8	occurred
6	2	.0076	8.2	1,208	.4190	.0446	353.6	at gages
6	3	.0114	8.4	1,252	.4269	.0525	530.4	7 & 20
6	4	.0152	8.4	1,256	.4282	.0538	707.2	
6	5	.0190	8.6	1,282	.4371	.0627	884.0	
6	8	.0304	9.1	1,364	.4650	.0906	1,414.4	
6	12	.0456	9.8	1,470	.5014	.1270	2,121.6	
6	16	.0608	10.1	1,495	.5099	.1355	2,828.8	
6	20	.0760	10.5	1,577	.5379	.1635	3,536.0	

TABLE I — Continued

e in	p psi	$\bar{p}$	P_{cr} kips	ϵ_{ucr} 10^{-6}	$\bar{\sigma}_{ucr}$	$\Delta\bar{\sigma}_{ucr}$	$p\pi r^2$ lbs	Remarks
8	0	.0000	6.2	1,440	.4910	.0000	0.0	buckling
8	1	.0038	6.4	1,489	.5077	.0167	176.8	occurred
8	2	.0076	6.6	1,528	.5209	.0299	353.6	at gages
8	3	.0114	6.8	1,586	.5409	.0499	530.4	7 & 20
8	4	.0152	6.9	1,608	.5484	.0574	707.2	
8	5	.0190	7.0	1,627	.5548	.0638	884.0	
8	8	.0304	7.1	1,647	.5617	.0707	1,414.4	
8	12	.0456	7.5	1,751	.5970	.1060	2,121.6	
8	16	.0608	7.8	1,825	.6224	.1314	2,828.8	
8	20	.0760	8.2	1,904	.6494	.1584	3,536.0	

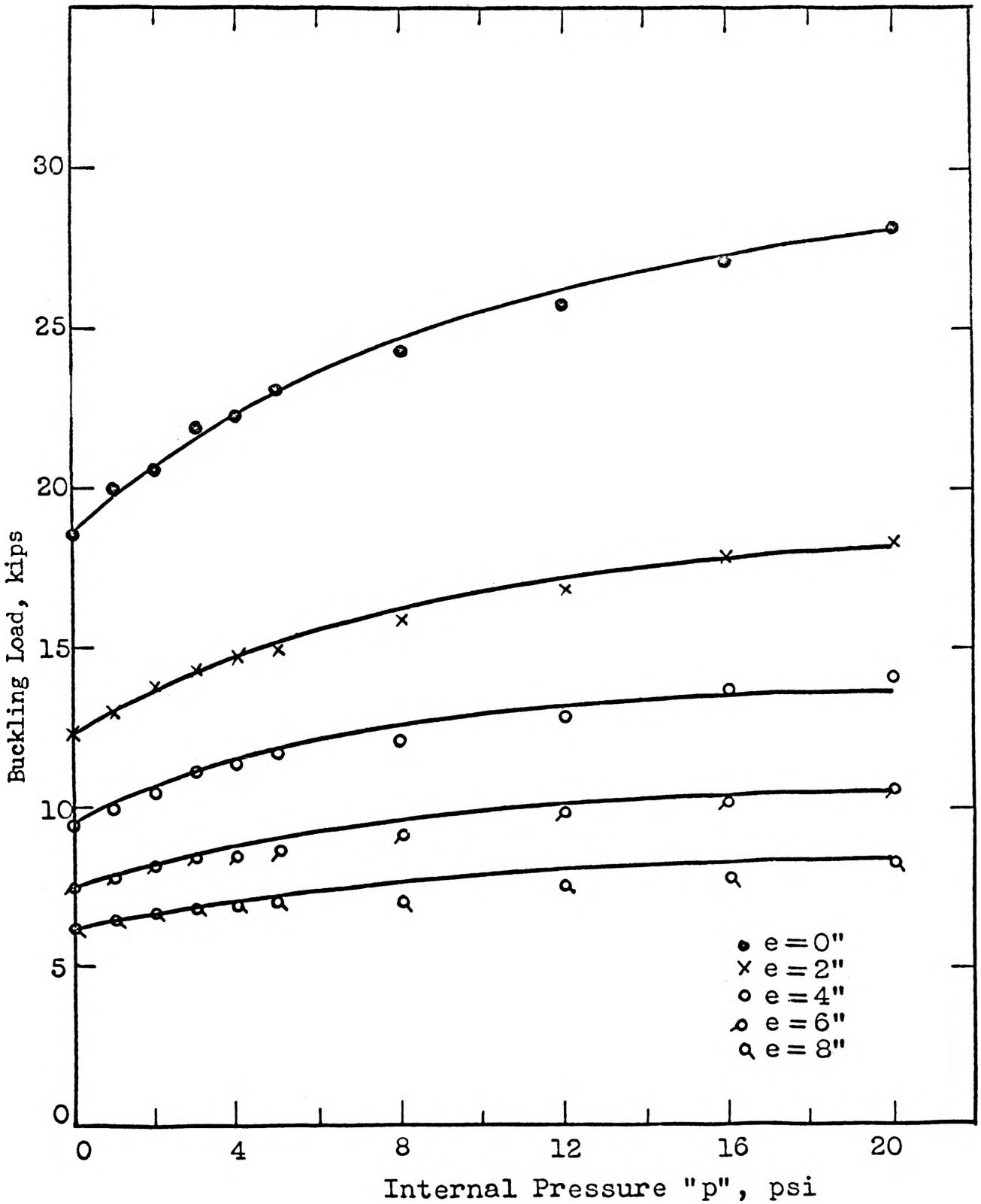

Fig. 11. Experimental values of the buckling load at various internal pressures at e = 0, 2, 4, 6, 8 inches respectively

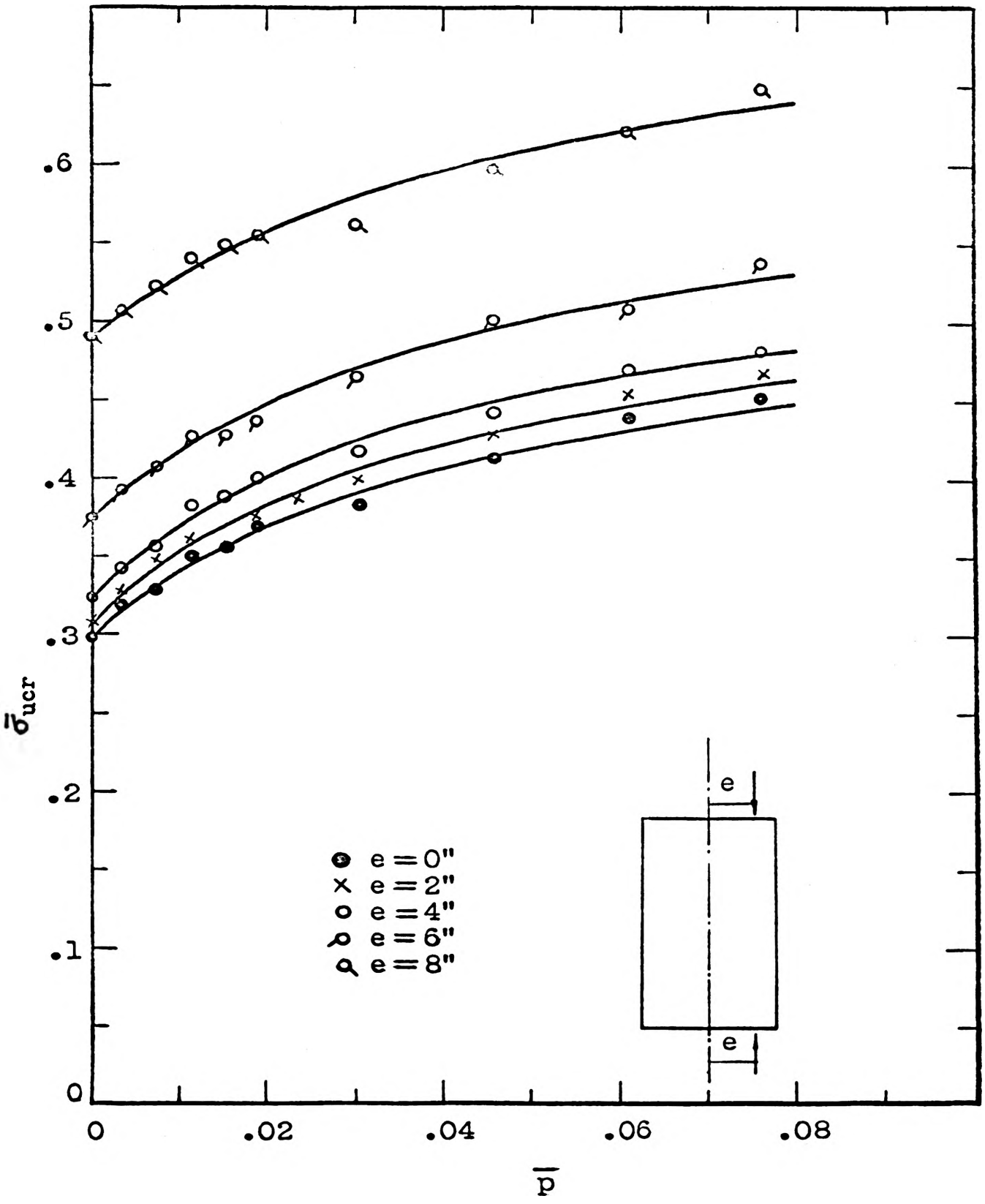

Fig. 12. Experimental values of the buckling stress at various internal pressures at e = 0, 2, 4, 6, 8 inches respectively

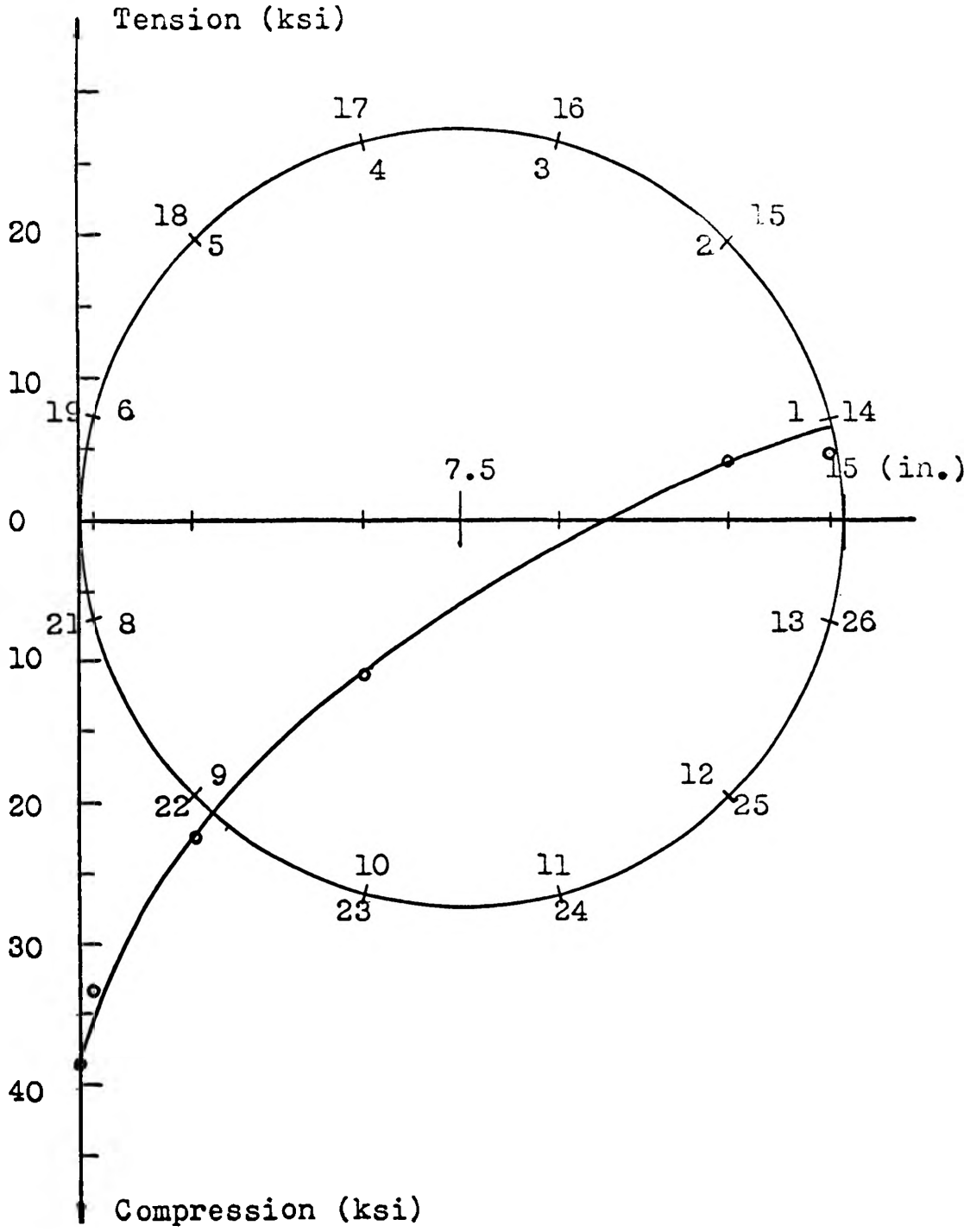

Fig. 13. Stress distribution at the mid-length of the cylinder when e = 6", p = 5 psig and P_{cr} = 8.6 kips

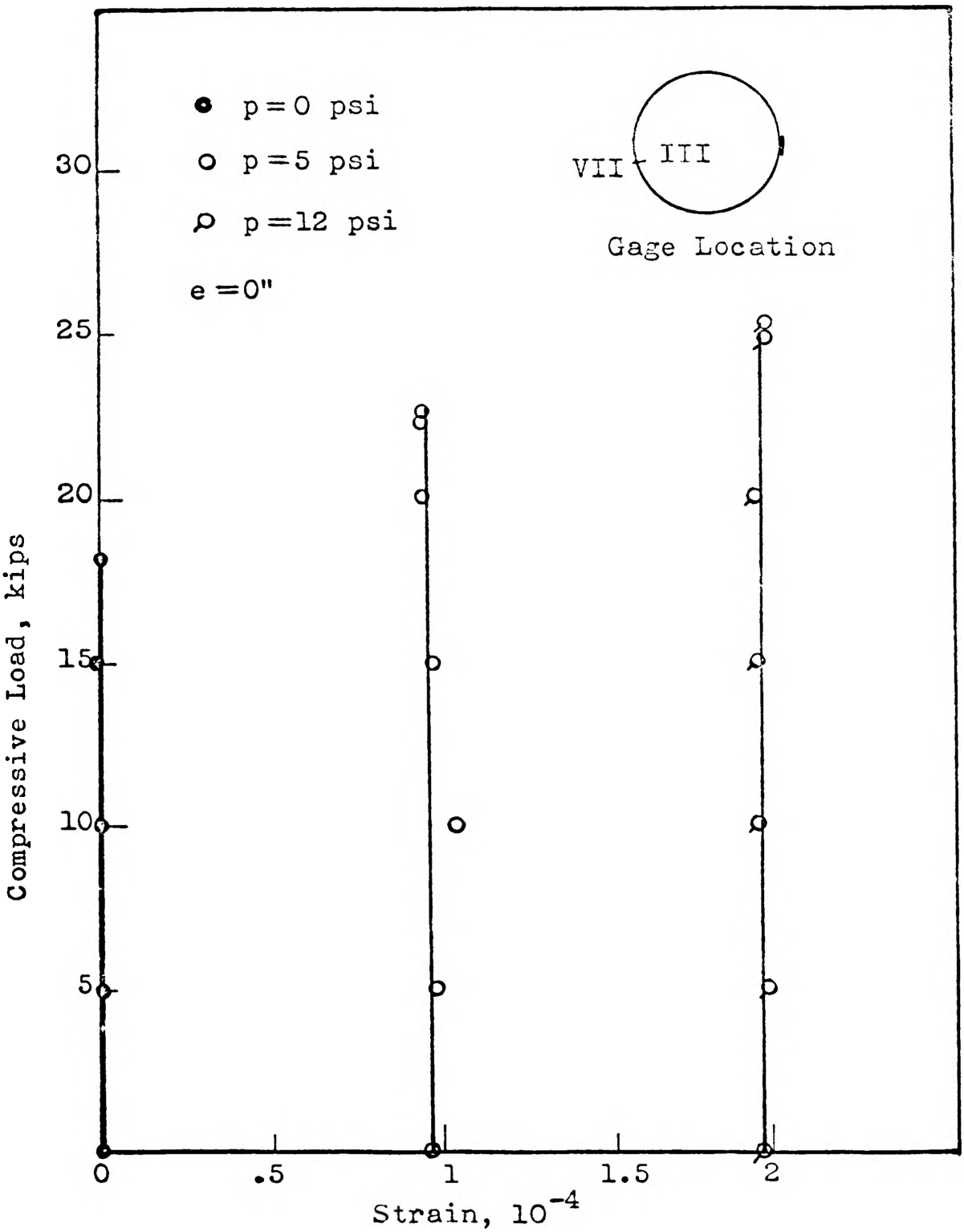

Fig. 14. Typical load-strain curve in the circumferential direction (gages III & VII)

Chapter IV

CONCLUSIONS

From the experimental results shown in Figs. 11 and 12, the internal pressure is seen to have an appreciable strengthening effect on the cylindrical shell. In Fig. 11 it shows that the buckling load of the shell decreases as the eccentricity increases and the effect of internal pressure to buckling load decreases with an increase of eccentricity. In Fig. 12, although the five curves obtained from the test results of the various eccentricities have their own characteristics, all of them still show the same trends in the effect of internal pressure on the buckling stress.

In Fig. 15, the increment of the buckling stress parameter due to the presence of internal pressure, $\Delta\bar{\sigma}_{ucr}$ or $\bar{\sigma}_{ucr} - (\bar{\sigma}_{ucr})_{\bar{p}=0}$, is plotted against the internal pressure parameter. The five curves of the various eccentricities can be seen to be in close agreement, in that the curves for $\Delta\bar{\sigma}_{ucr}$ are nearly the same for all eccentricities. These data indicate that, although further refinement may be necessary for exact determination of the magnitudes of the compressive buckling stresses, the common trend of the five curves gives a fairly good prediction of the increase of compressive

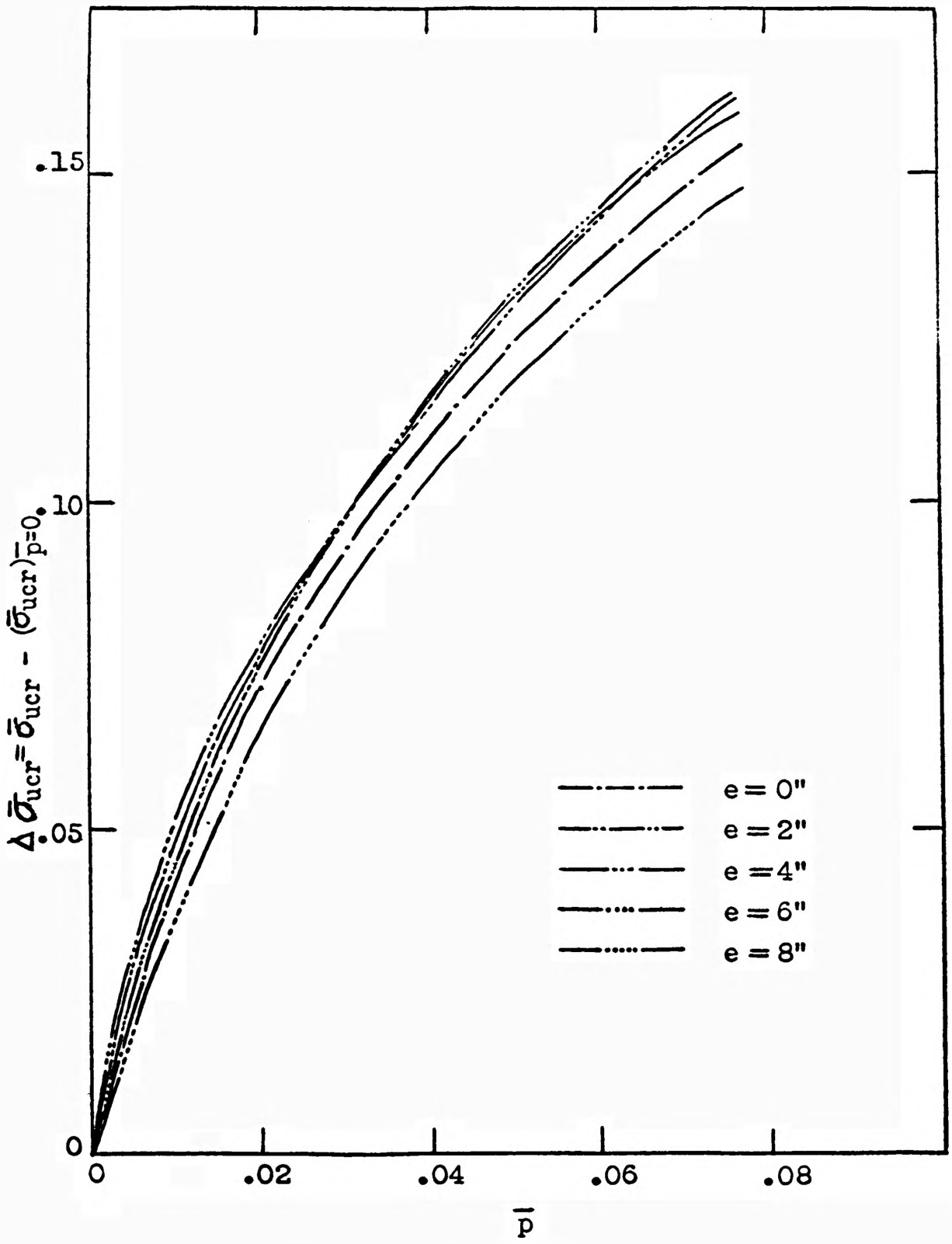

Fig. 15. Experimental results showing the increment of buckling stress ($\Delta\bar{\sigma}_{ucr}$) due to internal pressures at various eccentricities

buckling stress due to internal pressures under different eccentricities.

The slight discrepancies among the curves in Fig. 15 are believed to be caused essentially by imperfections of the test and possible theoretical considerations.

In Fig. 13, the stress distribution curve of the cylindrical shell shows that the straight-line theory cannot be applied to the shell problem.

From the test results shown in Fig. 14, the stress in the circumferential direction is mainly a function of internal pressure and does not depend on loading.

Chapter V

RECOMMENDATIONS

Since only one specimen was used in this study, a further investigation should be made if the determination of the magnitudes of buckling stress is desired.

The author would like to recommend not only specimens with different dimensions but with different materials should be tested to determine the effects of length-diameter ratio, thickness of wall and the material properties.

Furthermore, in order to obtain more detailed information on the shell problem, experiments using torsion as well as eccentric and axial loading should be conducted.

BIBLIOGRAPHY

1. S. P. TIMOSHENKO and J. M. GREE, Theory of Elastic Stability, McGraw-Hill Book Co., Inc., New York, New York, 1961.

2. J. P. DEN HARTOG, Advanced Strength of Materials, McGraw-Hill Book Co., Inc., New York, New York, 1952.

3. H. LO, H. CRATE and E. B. SCHWARTZ, "Buckling of Thin-walled Cylinder under Axial Compression and Internal Pressure", NACA Technical Note 2021, Washington, January, 1950.

4. P. SEIDE, V. I. WEINGARTEN and E. J. MORGAN, "Final Report on the Development of Design Criteria for Elastic Stability of Thin Shell Structures", Space Technology Laboratory, Inc., Los Angeles, Calif., prepared for Air Force Ballistic Missile Division, Air Research and Development Command, USAF, Inglewood, Calif, December, 1960.

5. M. B. DOW and J. P. PETERSON, "Bending and Compression Tests of Pressurized Ring-Stiffenced Cylinders", NASA Technical Note D-360, Washington, April, 1960.

6. RAFEL and NORMAN, "Effect of Normal Pressure on the Critical Compressive Stress of Curved Sheet", NACA RB, November, 1942.

7. G. W. ZENDER, "The Bending Strength of Pressurized Cylinders", Journal of the Aerospace Science, Vol 29, No. 3, March, 1962.

8. W. FLUGGE, "Die Stabilitat der Krieszylinderschale", Ing.-Archiv, Bd. III, Heft 5, December, 1932.

VITA

Chao-Ping Chu, son of Mr. and Mrs. Yu-Mei Chu, was born on January 14, 1939 at Chengtu, Szchwan, China, where he completed a part of his elementary education.

In 1945, after the Sino-Japanese War, he went to Nanking, the capital of China; and to Taiwan in 1949 where he completed his elementary education the following year. In June 1956 he graduated from the High School of Taiwan Normal University; and the same year he attended Taiwan Christian College, where he received his B. S. degree in Civil Engineering in June 1960.

After more than one year's military service and two years' practice in Taiwan, he enrolled as a graduate student in the Department of Civil Engineering of the University of Missouri School of Mines and Metallurgy, Rolla, Mo. in September 1963.

On June 27, 1964, in Massachusetts, he was married to Liang-Fong Hsiao of China.